SWIMMING OF FLAGELLATED MICROORGANISMS

JOSEPH B. KELLER *and* S. I. RUBINOW

From the Courant Institute of Mathematical Sciences, New York University, New York 10012, and the Graduate School of Medical Sciences, Cornell University, New York 10021

ABSTRACT The swimming motion of a microorganism with a single flagellum is investigated for both helical and planar flagellar motion. First the force and torque exerted on the organism by the surrounding fluid are calculated in terms of the specified flagellar motion and the unknown linear and angular velocity of the whole organism. Then these unknown velocities are determined by the condition that the net force and torque on the organism are zero. Using these velocities, the trajectory of the organism is found. In the case of helical flagellar motion, the path of the entire organism is found to be a helix of small radius. The axis of the flagellum is not parallel to the axis of the helical path, but makes a small angle with it and precesses around it. If the flagellar motion is planar and sinusoidal, then the trajectory of the organism is found to be a straight line with small oscillations about it. Each point of the flagellum also oscillates longitudinally with double the frequency of the transverse oscillation, producing a figure eight motion. However if the flagellar motion is planar and asymmetric, then the trajectory is found to be a circle with small superposed oscillations. These conclusions account for the observed helical and circular trajectories of sperm, and for the figure eight motion of the tip of the flagellum in the planar case.

1. INTRODUCTION

Some microorganisms, such as sperm, possess single flagella containing contractile elements. By using them, an organism can send periodic bending waves along its flagellum away from its head. In this way, it can propel itself head first through the surrounding fluid. Two types of flagellar wave motion have been observed, helical and planar, with two corresponding types of trajectories of the organisms. In the case of helical flagellar motion, the trajectory is practically a straight line with a small helical motion about it (Buller, 1903; Rothschild and Swann, 1949; Gray, 1955; Rikmenspoel et al., 1960). In the case of planar flagellar motion, the trajectory is a circle (Buller, 1903; Gray, 1955; Rikmenspoel et al., 1960; Rothschild and Swann, 1950; Brokaw, 1965). Our objective is to provide a theoretical explanation of those aspects of these trajectories which have not been explained before, together with a quantitative description of them.

The early analysts of helical flagellar motion determined the longitudinal component of linear velocity $\mathbf{w}$ of the organism, assuming that the angular velocity Ω was given (Taylor, 1952; Hancock, 1953; Holwill and Burge, 1963). Chwang and Wu (1971) improved upon this by calculating the longitudinal components of both $\mathbf{w}$ and Ω. These

previous calculations yielded straight line trajectories for the organism. We shall calculate the transverse as well as the longitudinal components of $\mathbf{w}$ and Ω, and use them to show that when the flagellum moves helically, the organism moves along a helical path of small radius. Furthermore, the axis of the flagellum is inclined at a small angle to the axis of the path and precesses about it. These results are in qualitative agreement with the observations referred to above.

Our analysis of helical flagellar motion yields the results of Chwang and Wu (1971) for the longitudinal components of $\mathbf{w}$ and Ω. We show how the result for the swimming velocity, which is the longitudinal component of $\mathbf{w}$, reduces to the results of Taylor and of Hancock in certain limiting cases. This eliminates an apparent disagreement between those results and that of Chwang and Wu. In addition, we have used the result for the longitudinal component of Ω to calculate the linear and angular velocities of a bull sperm with a helically waving flagellum, observed by Rikmenspoel et al. (1960). The agreement is at best fair.

In the case of planar flagellar motion, the early investigators also confined their analyses to the determination of the longitudinal component of $\mathbf{w}$. Then Brokaw (1970) showed how to calculate both components of $\mathbf{w}$ and the single component of Ω for arbitrary planar motion of the flagellum. His equations, rederived by Shack et al. (1974), were employed by Brokaw (1970, 1971) and by Yundt et al. (1975). They used smoothed numerical representations of observed flagellar motions as the input, and calculated numerically $\mathbf{w}$ and Ω, as well as the bending moment on the flagellum. In addition Brokaw (1971) calculated the bending moment analytically, and Shack et al. (1974) calculated $\mathbf{w}$ and Ω analytically, for small amplitude sinusoidal flagellar motion. We shall show that the latter result, and a more general one which we derive, yield transverse oscillations about the mean trajectory, such as were observed by Rothschild and Swann (1950) in the motion of the heads of sea urchin sperm.

Despite the thoroughness of the studies of planar flagellar motion just referred to, there are still some aspects of the observed motions which have not been explained adequately. One of these is the fact that the mean trajectory is circular rather than straight (Gray, 1955; Rikmenspoel et al., 1960). Furthermore its radius of curvature is smaller when the asymmetry of the flagellar motion is larger (Rikmenspoel et al., 1960). This clearly shows that the circular path is a result of the asymmetry, as Brokaw (1970) pointed out. Another unexplained observation is the figure eight motion displayed by the tip of a flagellum during one cycle of the wave motion (Gray, 1958). A third is the observation of Rikmenspoel (1965) on bull sperm with planar flagellar motions, in which the observed swimming velocities differ by a factor of five from the calculated values based upon the formula of Gray and Hancock (1955) (Fig. 1).

We shall indicate how the circular paths can be accounted for, explain the figure eight motion, and recalculate the bull sperm velocities in an improved way, obtaining much better agreement with the observed values.

In the next section we shall determine $\mathbf{w}$ and Ω in terms of $\mathbf{F}'$ and $\mathbf{T}'$, the propulsive force and torque due to the motion of some parts of the organism relative to other

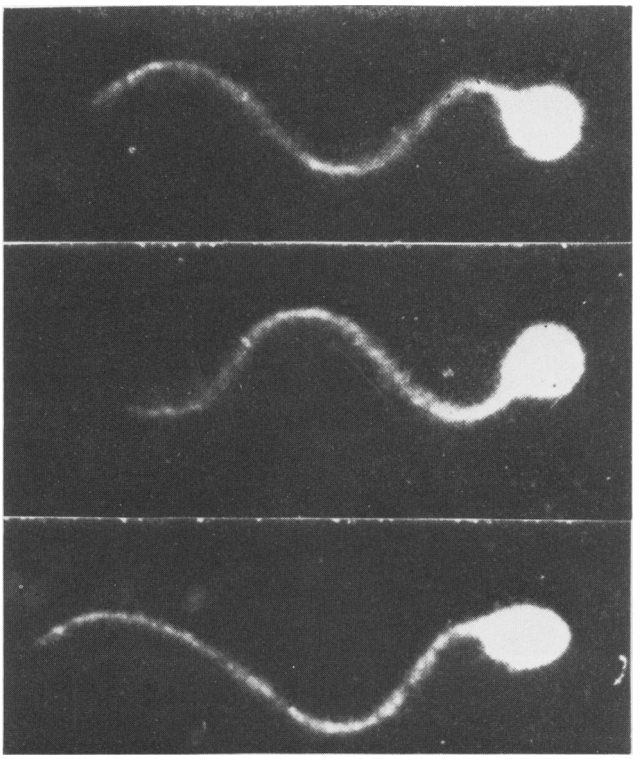

FIGURE 1 Photographs of three sea urchin sperm (*Psammechinus miliaris*) in approximately planar sinusoidal motion, taken from Gray (1955).

parts, and the drag coefficient matrix G. In sections 3 and 4 we shall calculate the trajectories for organisms with planar and helical flagellar motions, respectively. In sections 5 and 6 we shall calculate G, $\mathbf{F}'$, and $\mathbf{T}'$ for these respective cases and use them to get explicit expressions for $\mathbf{w}$ and Ω.

2. DETERMINATION OF $\mathbf{w}$ AND Ω

The fluid motion which results from the flagellar movement is very slow, having a Reynolds number of 10^{-3} or less. Therefore the theory of slow flow is applicable to it. This theory shows that the force $\mathbf{F}$ and torque $\mathbf{T}$ exerted by the fluid on the organism can be separated into propulsive and drag parts:

$$\begin{pmatrix}\mathbf{F}\\ \mathbf{T}\end{pmatrix} = \begin{pmatrix}\mathbf{F}'\\ \mathbf{T}'\end{pmatrix} - G\begin{pmatrix}\mathbf{w}\\ \Omega\end{pmatrix}. \tag{1}$$

Here G is the drag coefficient matrix, a nonsingular sixth order matrix. If there are no other forces or torques applied to the organism, then $\mathbf{F}$ and $\mathbf{T}$ must vanish. Upon setting $\mathbf{F} = \mathbf{T} = 0$ in Eq. 1, and solving for $\mathbf{w}$ and Ω, we obtain

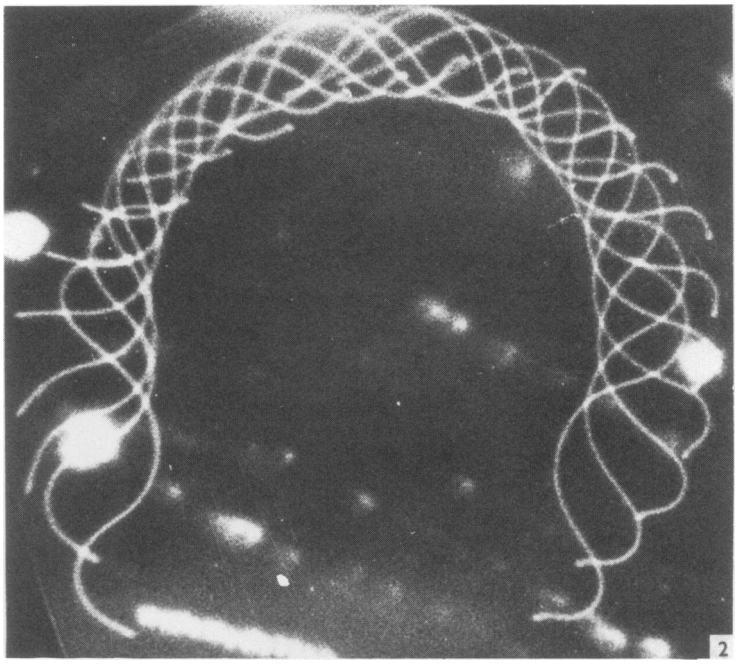

FIGURE 2 Multiple exposure of a headless sperm executing approximately planar sinusoidal motion. The flagellum is moving in a clockwise direction. The exposure frequency was slightly less than the frequency of oscillation. The path is nearly circular. From Brokaw (1970).

$$\begin{pmatrix} \mathbf{w} \\ \boldsymbol{\Omega} \end{pmatrix} = G^{-1} \begin{pmatrix} \mathbf{F}' \\ \mathbf{T}' \end{pmatrix}. \tag{2}$$

An immediate consequence of Eq. 2 is that in the absence of relative motion, in which case $\mathbf{F}' = \mathbf{T}' = 0$, we have $\mathbf{w} = \boldsymbol{\Omega} = 0$. Thus if the organism moves as a rigid body, it cannot swim. Now a helical wave motion of a flagellum is a rigid body motion. Therefore a single helically waving flagellum cannot swim unless it is attached to a head which moves relative to it. This explains the result of Chwang and Wu (1971) that a helically waving flagellum without a head cannot swim. However, if it is attached to a head, and if the head and flagellum rotate with different angular velocities, it can swim. On the other hand, a planar sinusoidal wave motion is not a rigid body motion. Therefore a headless flagellum executing such a motion can and does propel itself (Brokaw, 1970), as illustrated in Fig. 2.

3. TRAJECTORY OF AN ORGANISM WITH A PLANAR FLAGELLAR MOTION

We shall now consider an organism with a flagellum which performs planar oscillations. We assume that the flagellum lies in the XZ plane of a laboratory-fixed coordinate system, and is of length $L + \delta$ (see Fig. 3). Along the distal portion or tail, of

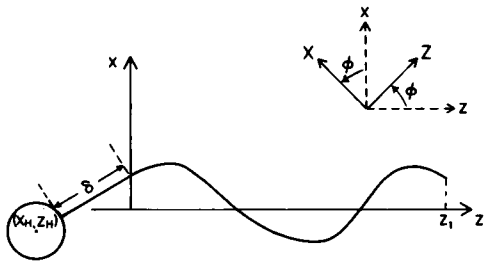

FIGURE 3

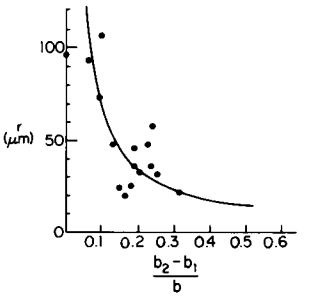

FIGURE 4

FIGURE 3 The body-fixed coordinate system for a sperm with a spherical head centered at the point (x_H, z_H), a midpiece of length δ, and a tail of length L lying in the xz plane. The z coordinates of the beginning and end of the tail are 0 and z_1, respectively. The laboratory-fixed coordinate system is rotated by an angle ϕ from the body-fixed system, as shown in the insert.

FIGURE 4 Each point indicates the radius of curvature r of the circular orbit of a sperm cell swimming with a planar tail motion which is slightly asymmetric. The abscissa $\epsilon = (b_2 - b_1)/b$ is a measure of this asymmetry. Here, b_1 is the amplitude of the oscillation on the inside of the circular orbit, b_2 is the amplitude on the outside, and $b = (b_1 + b_2)/2$. The solid line is based on the theoretical relation $r = A/\epsilon$. To fit the data, the constant A was chosen to equal 0.7 μm. The experimental points are taken from Rikmenspoel et al. (1960).

length L, a nearly sinusoidal wave travels in the distal direction with frequency ω and wavenumber k. Thus in a body-fixed coordinate system (x, y, z), the position vector $\mathbf{r}(s, t)$ of the point at distance s along this segment at time t is

$$\mathbf{r}(s, t) = [\rho \cos\theta + \epsilon(z, t), 0, z]. \tag{3}$$

Here $\epsilon(z, t)$ describes the small asymmetry of the motion, while θ and z are related to s and t by

$$\theta = kz - \omega t, \tag{4}$$

$$s(z, t) = \int_0^z [1 + k^2\rho^2 \sin^2(kz' - \omega t)]^{1/2} dz' + 0(\epsilon)$$

$$= k^{-1} \int_{-\omega t}^{\theta} [1 + k^2\rho^2 \sin^2\theta']^{1/2} d\theta' + 0(\epsilon). \tag{5}$$

The asymmetry of the tail motion has been observed repeatedly, but the asymmetrical part $\epsilon(s, t)$, has not been determined quantitatively. Therefore we shall not make use of its explicit form herein. The proximal segment or midpiece, of length δ, connects the point $\mathbf{r}(0, t)$ to the head, which is a sphere of radius R with center at $\mathbf{r}_H = (x_H, 0, z_H)$. Superposed on the oscillation is a rigid body motion with linear velocity $\mathbf{w} = (w_1, 0, w_3)$ in the xz plane of the body-fixed coordinate system, and with angular velocity $\Omega = (0, \Omega, 0)$ along the y axis.

In order to describe the motion of the organism in the laboratory coordinate system, we let $\mathbf{R}_o(t) = [X_o(t), Z_o(t)]$ denote the position of the origin of the body-fixed

coordinate system. We also let $\phi(t)$ be the angle between the x and X axes (see Fig. 3), and assume that the y and Y axes are parallel. Then in the lab system the velocity of the origin of the body-fixed system is

$$\frac{d\mathbf{R}_o}{dt} = \begin{bmatrix} \cos\phi(t) & \sin\phi(t) \\ -\sin\phi(t) & \cos\phi(t) \end{bmatrix} \begin{bmatrix} w_1 \\ w_3 \end{bmatrix}. \tag{6}$$

The angular velocity of the organism in the laboratory system is also Ω, which has just a Y component Ω, so $d\phi/dt = \Omega$.

In section 5, we show that for small ρ/L and small ϵ, the leading term in w_3 is a constant, the corresponding term in w_1 is zero, and the leading term in Ω is a constant of order ϵ. By using just these leading terms in the above equations, and choosing $\phi(0) = 0$ and $\mathbf{R}_o(0) = 0$, we get $\phi(t) = \Omega t$ and

$$\mathbf{R}_o(t) = (w_3/\Omega)[-\cos\Omega t, \sin\Omega t]. \tag{7}$$

This is the equation of a circle of radius w_3/Ω. The linear velocity w_3 along this circle is given by Eq. 29.

We see from Eq. 7 that the radius of the circle is inversely proportional to the asymmetry ϵ, since Ω is proportional to ϵ. This conclusion is in agreement with the observations of Rikmenspoel et al. (1960) shown in Fig. 4. The abscissa is a measure of the asymmetry ϵ, and the ordinate is the radius of the circle. The solid curve is a hyperbola of the form radius = const./asymmetry, in accordance with the prediction (Eq. 7), with the constant adjusted to make the curve pass through the observed points. By specifying the exact form of the asymmetric motion, it would be possible to calculate the constant theoretically.

From Eqs. 3 and 4 we see that in the body-fixed coordinate system, the x component of $\mathbf{r}(s, t)$ is essentially periodic in t with angular frequency ω. However from Eqs. 3 and 5 or 22 we see that the z component of $\mathbf{r}$ is essentially periodic in t with angular frequency 2ω. Thus each point of the flagellum performs a figure eight motion in the xz plane. This kinematic effect is in agreement with Gray's (1958) observation of the motion of the tip of the flagellum in the planar case.

4. TRAJECTORY OF ORGANISM WITH HELICAL FLAGELLAR MOTION

Let $\mathbf{r} = (x, y, z)$ be the cartesian coordinate vector in a system fixed in an organism with a helically waving flagellum. The z axis is along the axis of the helix, with the positive direction from head to tail (see Fig. 5). In this coordinate system G, $\mathbf{F}'$ and $\mathbf{T}'$, which were defined in section 1, are constants independent of t. This is shown in section 6 and Appendix B. Therefore from Eq. 2 it follows that $\mathbf{w}$ and Ω are also constants in this coordinate system. We denote their components by w_1, w_2, w_3 and $\Omega_1, \Omega_2, \Omega_3$, respectively. The equation of the helix is

$$\mathbf{r}(s) = [\rho\cos(ks\cos\beta), \rho\sin(ks\cos\beta), s\cos\beta]. \tag{8}$$

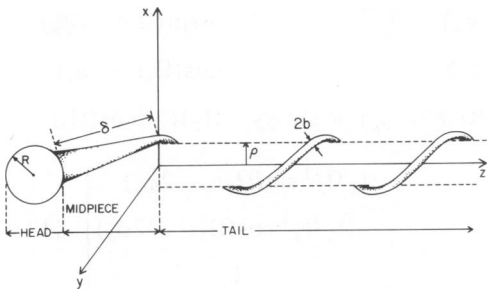

FIGURE 5 The body-fixed coordinate system of a sperm with a spherical head of radius R, a thick midpiece of length δ, and a tail which is executing helical motion about the z axis. The amplitude of the helical motion is ρ, and the thickness of the tail is $2b$. The z coordinates of the beginning and end of the tail are 0 and z_1, respectively. The end of the tail is not shown.

Here ρ is the amplitude, k is the wavenumber, and β is the pitch angle of the helix, while s is arclength along it.

In order to determine the trajectory of the organism, we introduce the coordinates $\mathbf{R} = (X, Y, Z)$ fixed in the laboratory. The transformation from $\mathbf{r}$ to $\mathbf{R}$ consists of a rotation $A^{-1}(t)$ which depends upon t, and a translation by an amount $\mathbf{R}_o(t)$. Then the equation of the helix in the laboratory system is

$$\mathbf{R}(s, t) = \mathbf{R}_o(t) + A^{-1}(t)\mathbf{r}(s). \tag{9}$$

The translation is determined by the equation

$$d\mathbf{R}_o/dt = A^{-1}(t)\mathbf{w}. \tag{10}$$

The matrix $A^{-1}(t)$ is expressible in terms of the Euler angles $\theta(t)$, $\phi(t)$ and $\psi(t)$ by Eqs. 4–47 of Goldstein (1950). The Euler angles in turn are determined by Ω via the differential equations (Goldstein, 1950), Eqs. 4–103:

$$\begin{aligned} \phi_t \sin\theta \sin\psi + \theta_t \cos\psi &= \Omega_1, \\ \phi_t \sin\theta \cos\psi - \theta_t \sin\psi &= \Omega_2, \\ \phi_t \cos\theta + \psi_t &= \Omega_3. \end{aligned} \tag{11}$$

In section 6 we shall show that Ω_1 and Ω_2 are both small compared with Ω_3. In this case the appropriate solution of Eq. 11 is

$$\begin{aligned} \theta(t) &= 2\Omega_\perp \Omega_3^{-1} \cos[(\Omega_3 t/2) - \phi_o] + 0(\Omega_\perp^2/\Omega_3^2), \\ \phi(t) &= (\Omega_3 t/2) - \phi_o + 0(\Omega_\perp/\Omega_3), \\ \psi(t) &= (\Omega_3 t/2) + 0(\Omega_\perp/\Omega_3). \end{aligned} \tag{12}$$

Here $\phi_o = \tan^{-1}\Omega_1/\Omega_2$ and $\Omega_\perp = (\Omega_1^2 + \Omega_2^2)^{1/2}$. We have chosen the initial value of ϕ so that the steady translation will turn out to be along the Z axis.

By using Eq. 12 in the equation for $A^{-1}(t)$ referred to above, we get

$$A^{-1}(t) = \begin{bmatrix} \cos(\Omega_3 t - \phi_o) & -\sin(\Omega_3 t - \phi_o) & \Omega_\perp \Omega_3^{-2} \sin(\Omega_3 t - 2\phi_o) \\ \sin(\Omega_3 t - \phi_o) & \cos(\Omega_3 t - \phi_o) & -\Omega_\perp \Omega_3^{-2} \cos(\Omega_3 t - 2\phi_o) \\ \Omega_\perp \Omega_3^{-1}[\sin(\Omega_3 t - \phi_o) + \sin\phi_o] & \Omega_\perp \Omega_3^{-1}[\cos(\Omega_3 t - \phi_o) + \cos\phi_o] & 1 \end{bmatrix} \{1 + 0(\Omega_\perp/\Omega_3)\}. \quad (13)$$

We now use Eq. 13 in 10, integrate, and rewrite the result in the form

$$R_o(t) = \begin{bmatrix} \Omega_3^{-2}(\Omega \times \mathbf{w})_\perp \cos(\Omega_3 t - \tau) \\ \Omega_3^{-2}(\Omega \times \mathbf{w})_\perp \sin(\Omega_3 t - \tau) \\ \Omega_3^{-1} \Omega \cdot \mathbf{w} t \end{bmatrix} \{1 + 0(\Omega_\perp/\Omega_3)\}. \quad (14)$$

Here $(\Omega \times \mathbf{w})_\perp$ is the length of the component of $\Omega \times \mathbf{w}$ perpendicular to the Z axis, τ is defined by

$$\tau = \tan^{-1} \frac{w_3 \Omega_\perp \sin(\gamma - \phi_o)}{\Omega_3 (w_1^2 + w_2^2)^{1/2} - w_3 \Omega_\perp \cos(\gamma - \phi_o)}, \quad (15)$$

and $\gamma = \tan^{-1} w_1/w_2$.

The result (Eq. 14) gives the trajectory $\mathbf{R}_o(t)$ of the origin of the body-fixed coordinate system, which we shall call the trajectory of the organism. It is a helix of radius $\Omega_3^{-2}(\Omega \times \mathbf{w})_\perp$ about the Z axis with period $2\pi(\Omega \cdot \mathbf{w})\Omega_3^{-2}$ along the Z axis and pitch angle $\tan^{-1}[(\Omega \times \mathbf{w})_\perp / \Omega \cdot \mathbf{w}]$. The velocity of the organism along the Z axis is $(\Omega \cdot \mathbf{w})/\Omega_3$. Furthermore the direction of the z axis, which is the axis of the flagellum, is determined by the last column of the matrix 13. This shows that the z axis makes the small angle $\Omega_\perp/\Omega_3$ with the Z axis, and precesses about it with angular velocity Ω_3.

To find the position of the flagellum in the laboratory system we first use Eqs. 8 and 13 to get $A^{-1}(t)\mathbf{r}(s)$. Then we use this and $\mathbf{R}_o(t)$, given by Eq. 14, in 9 to obtain the result

$$\mathbf{R}(s,t) = \begin{bmatrix} \Omega_3^{-2}(\Omega \times \mathbf{w})_\perp \cos(\Omega_3 t - \tau) + q\cos(\Omega_3 t + ks\cos\beta - \phi_o - \sigma) \\ \Omega_3^{-2}(\Omega \times \mathbf{w})_\perp \sin(\Omega_3 t - \tau) + q\sin(\Omega_3 t + ks\cos\beta - \phi_o - \sigma) \\ \Omega_3^{-1} \Omega \cdot \mathbf{w} t + s\cos\beta \end{bmatrix} + \cdots \quad (16)$$

Here q and σ are defined by

$$q^2 = \rho^2 + (\Omega_\perp ks\cos\beta/\Omega_3)^2 - (2\Omega_\perp \rho ks\cos\beta/\Omega_3)\cos(ks\cos\beta + \phi_o), \quad (17)$$

$$\sigma = \tan^{-1}\{\Omega_3^{-1}\Omega_\perp ks\cos\beta\cos(ks\cos\beta + \phi_o) \cdot [\rho - \Omega_3^{-1}\Omega_\perp ks\cos\beta\sin(ks\cos\beta + \phi_o)]^{-1}\}. \quad (18)$$

The result (Eq. 16) shows that each point of the flagellum moves along a helical trajectory. This disagrees with Rikmenspoel's (1965) observation that the transverse motion of a point on the flagellum is the sum of two sinusoidal oscillations with unequal frequencies.

5. FORCE, TORQUE, AND VELOCITIES FOR PLANAR MOTION

The force **F** and torque **T** on the flagellum can be calculated if the flagellum is slender and if the motion is slow. Let b denote the radius of the circular cross section of the flagellum. Thus the slenderness ratio b/L and the Reynolds number must both be small. In this case the work of Cox (1970) yields, neglecting terms of order $(\log b/L)^{-2}$ and of order of the square of the Reynolds number,

$$\mathbf{F} = -\frac{2\pi\mu}{\log(b/\alpha L)} \int_0^L \mathbf{v} \cdot \left[\frac{d\mathbf{r}}{ds}\frac{d\mathbf{r}}{ds} - 2I\right] ds, \tag{19}$$

$$\mathbf{T} = -\frac{2\pi\mu}{\log(b/\alpha L)} \int_0^L \mathbf{r} \times \left(\mathbf{v} \cdot \left[\frac{d\mathbf{r}}{ds}\frac{d\mathbf{r}}{ds} - 2I\right]\right) ds. \tag{20}$$

Here μ is the viscosity of the fluid, s is arclength along the flagellum, $\mathbf{r}(s,t)$ is the equation of the flagellum, $\mathbf{v}(s,t) = \mathbf{w} + \Omega \times \mathbf{r} + \mathbf{r}_t$ is the velocity of the flagellum, and α is a numerical coefficient. The results 19 and 20 are essentially the same as those predicated by Gray and Hancock (1955). They were applied to the planar case by Brokaw (1970). The following analysis differs from his in that it is analytical rather than numerical, so it is based upon an idealized wave motion rather than an observed one.

By using Eqs. 3 and 4 in the above expression for $\mathbf{v}$, and neglecting terms of order ϵ, we obtain for $\mathbf{v}$ in the planar case

$$\mathbf{v}(s,t) = [\rho(\omega - kz_t)\sin(kz - \omega t), 0, z_t] + (w_1 + \Omega z, 0, w_3 - \rho\Omega\cos\theta). \tag{21}$$

The velocity z_t is found, by differentiating Eq. 5, to be

$$z_t = c - c(1 + k^2\rho^2\sin^2\omega t)^{1/2}(1 + k^2\omega^2\sin^2\theta)^{-1/2}, \tag{22}$$

where $c = \omega/k$ is the phase velocity of the wave. From Eqs. 3 and 5 we also get

$$d\mathbf{r}/ds = (1 + k^2\rho^2\sin^2\theta)^{-1/2}(-k\rho\sin\theta, 0, 1). \tag{23}$$

We now substitute these expressions into Eqs. 19 and 20. We write the three nonzero components F_1, F_3, and T in the form

$$\begin{bmatrix} F_1 \\ F_3 \\ L^{-1}T \end{bmatrix} = \frac{2\pi\mu L}{\log(b/\alpha L)} G^{\rho} \begin{bmatrix} w_1 \\ w_3 \\ L\Omega \end{bmatrix} + \begin{bmatrix} F_1^r \\ F_3^r \\ L^{-1}T^r \end{bmatrix}. \tag{24}$$

The drag matrix G^p and the force and torque $\mathbf{F}^r$ and $\mathbf{T}^r$ due to the relative motion are given in Appendix A.

We now add $\mathbf{F}$ to the force $-6\pi\mu R\mathbf{w}$ on the head, assumed to be a sphere of radius R, and equate the sum to zero. Similarly we set

$$\mathbf{T} - 8\pi\mu R^3\Omega + \mathbf{r}_H \times (-6\pi\mu R\mathbf{w})$$

equal to zero. In this way we get the three equations

$$\frac{2\pi\mu L}{\log(b/\alpha L)} G^p \begin{pmatrix} w_1 \\ w_3 \\ L\Omega \end{pmatrix} - 2\pi\mu R \begin{pmatrix} 3w_1 \\ 3w_3 \\ 4L^{-1}R^2\Omega + 3L^{-1}z_H w_1 \\ \quad - 3L^{-1}x_H w_3 \end{pmatrix} = -\begin{pmatrix} F_1^r \\ F_3^r \\ L^{-1}T^r \end{pmatrix}. \quad (25)$$

To solve Eq. 25 for w_1, w_3, and Ω we shall simplify it for a tail of length L large compared with ρ. It turns out that w_1/c and $L\Omega/c$ are both $0(\rho/L)$. The time average of the $0(\rho/L)$ terms in w_1 and Ω is zero. As a consequence of the oscillatory nature of w_1, the trajectory of the organism is a circle with small radial oscillations. Such oscillations are observed in the tracks of sea urchin sperm, which have been photographed with time exposures lasting 1/2 s (Rothschild and Swann (1950)), as shown in Fig. 6.

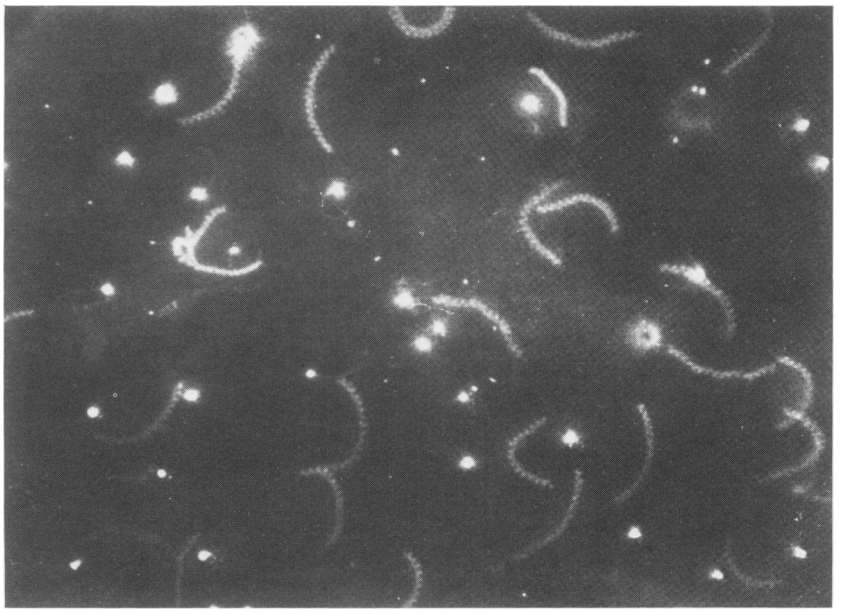

FIGURE 6 Photograph of many sea urchin sperm cells executing planar motion. The exposure time was 1/2 s. The sperm tails are too small and their motion was too rapid to be recorded by this exposure. The observed tracks are made by the heads of the sperm cells. These tracks indicate that the sperm trajectories are approximately circular, with small radial oscillations superposed. From Rothschild and Swann (1950).

The term in Ω of order ϵ, which we have not computed, has a nonzero average value. Upon neglecting all terms of order Ω/L, we find that Eq. 25 reduces to just one equation for w_3. Its solution is

$$w_3 = -\left[\frac{2\pi\mu L}{\log(b/\alpha L)} G^p_{22} - 6\pi\mu R\right]^{-1} F'_3. \tag{26}$$

By using the expressions for G^p_{22} and F'_3 in Appendix A, we can write Eq. 26 in the form

$$\frac{w_3}{c} = -\frac{2 - (z_1/L)(1 + k^2\rho^2\sin^2\omega t)^{1/2} - (1/kL)\displaystyle\int_{\omega t}^{\theta_1} (1 + k^2\rho^2\sin^2\theta)^{-1/2}\mathrm{d}\theta}{2 - (1/kL)\displaystyle\int_{-\omega t}^{\theta_1} (1 + k^2\rho^2\sin^2\theta)^{-1/2}\mathrm{d}\theta - (3R/L)\log(b/\alpha L)}. \tag{27}$$

Here $\theta_1 = kz_1 - \omega t$ and z_1 is determined by Eq. 5 with $s = L$, which becomes

$$kL = \int_{-\omega t}^{kz_1 - \omega t} (1 + k^2\rho^2\sin^2\theta)^{1/2}\mathrm{d}\theta. \tag{28}$$

Eq. 27 is a new result for the instantaneous z-component of the swimming velocity of a flagellated microorganism whose tail is performing planar sinusoidal transverse bending waves. The integrals appearing in Eqs. 27 and 28 can be expressed in terms of incomplete elliptic integrals of the first and second kind, respectively.

It follows from Eqs. 27 and 28 that w_3 and z_1 are periodic in t with angular frequency 2ω. Since the x-coordinate of the end has angular frequency ω while z_1 has frequency 2ω, the end point performs a figure eight motion. In Fig. 7 we show kz_1 as a function of ωt over one half-period, obtained by numerical calculation from Eq. 28, for $k\rho = 1$, $kL = 1.4$, and $R/L = 0$, which are representative values for headless sea urchin (*Psammechinus miliaris*) sperm. The average value of kz_1, denoted by

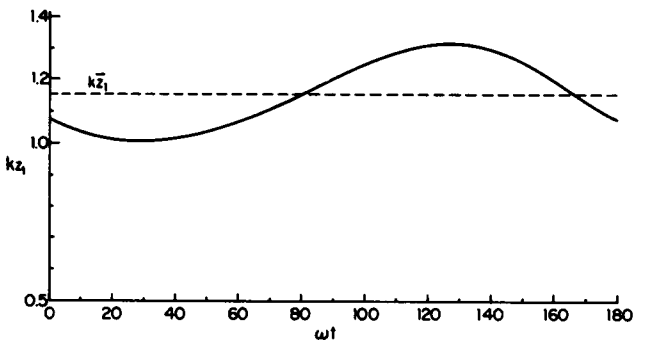

FIGURE 7 The quantity kz_1 is shown as a function of ωt in radians, over one half-period. Here z_1 is the z coordinate of the end point of a tail executing planar sinusoidal motion. The curve is based on Eq. 28 with $k\rho = 1$ and $kL = 1.4$. The mean value $\overline{kz_1}$ is shown as a dotted line.

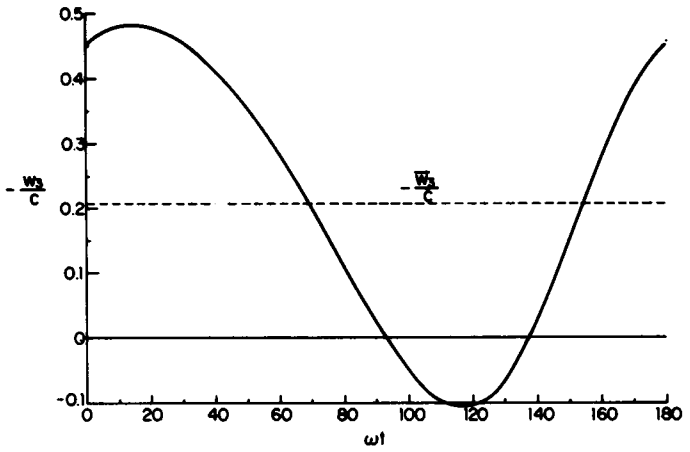

FIGURE 8 The velocity $-w_3$ divided by the phase velocity c is shown as a function of ωt in radians, for a headless sperm. The tail is executing planar sinusoidal motion. The curve is based on Eq. 27 with $k\rho = 1$ and $kL = 1.4$. The mean value $-\bar{w}_3/c$ is shown as a dotted line.

$k\bar{z}_1$, is also shown. In Fig. 8 we show $-w_3/c$ as a function of ωt over one half-period, for the same parameter values, obtained from (27). The average value $-\bar{w}_3/c$ is also shown. It is interesting to note that $-w_3$ is positive over most of its period, but that it is slightly negative over a short interval, which means that the organism is moving backwards during this short interval. At this time, the organism is nearly straight, since its projection on the z-axis is near its maximum length. This can be seen from the curve of the end point z_1 as a function ωt, shown in Fig. 7.

A crude formula for $\bar{w}_3$ can be obtained from Eqs. 27 and 28 by replacing $\sin^2\theta$ and $\sin^2\omega t$ by 1/2, which is the average value of $\sin^2\theta$ over one period. Then Eq. 27 yields

$$-\frac{\bar{w}_3}{c} \approx \frac{k^2\rho^2/2}{1 + k^2\rho^2 - [1 + (k^2\rho^2/2)](3R/L)\log(b/\alpha L)}. \tag{29}$$

With the appropriate value of α, this is just the result of Gray and Hancock (1955). For $k\rho = 1$ and $R/L = 0$, Eq. 29 yields $-\bar{w}_3/c = 0.25$, while the numerical calculation from Eq. 27 yields the correct value $-\bar{w}_3/c = 0.209$. Thus, the approximate formula of Gray and Hancock yields a value of $-\bar{w}_3/c$ which is about 20% too large. A similar conclusion was reached by Shack et al. (1974). A better approximate formula results if $\sin^2\theta$ and $\sin^2\omega t$ in Eqs. 27 and 28 are replaced by the value 0.36. Then Eq. 27 becomes

$$-\frac{\bar{w}_3}{c} \approx \frac{0.36k^2\rho^2}{1 + 0.72k^2\rho^2 - (1 + 0.36k^2\rho^2)(3R/L)\log(b/\alpha L)}. \tag{30}$$

When $R = 0$ and $k\rho = 1$, this formula yields the result $-\bar{w}_3/c = 0.209$, which is the same value as that determined from Eq. 27.

TABLE I

COMPUTED AND OBSERVED $-\bar{w}_3$

Cell no.	$-\bar{w}_3$(calc.)	$-\bar{w}_3$(obs.)
	$\mu m/s$	$\mu m/s$
1	81	60
2	104	70
3	95	77
4	53	80
5	100	82
6	94	105

We have used Eq. 30 to calculate the velocities $\bar{w}_3$ for six bull sperm whose motions were observed by Rikmenspoel et al. (1960). From their data we took $b = 0.4\ \mu$m and $R = 4\ \mu$m, the latter being an effective radius of an ellipsoidal head with axes 8, 4, and 1 μm, together with an attached thick midpiece. From supplementary data in Fig. 5 of Rikmenspoel (1965), we inferred that $z_1 = 45\ \mu$m. In Table I he gave the values of ρ, $\omega/2\pi$, and $2\pi/k$ for each sperm cell. Then Eq. 28 and the approximation $\sin^2\theta \approx 0.36$ yielded L for each sperm. We also used Gray and Hancock's (1955) estimate $\alpha L \approx 4\pi/ke^{1/2}$, and the relation $c = \omega/k$. With these data we computed $-w_3$ for each sperm cell. The results are shown in Table I, together with the observed velocities. We see that the calculated values are in error by about 30%. This discrepancy is much less than the factor of five reported by Rikmenspoel et al. (1960).

6. FORCE, TORQUE AND VELOCITIES FOR HELICAL MOTION

We choose as a model of a swimming microorganism with a helically moving flagellum that shown in Fig. 5. It consists of a spherical head of radius R attached to a flagellum of length $L + \delta$ and circular cross section of radius b. The tail or distal segment of length L forms a helix of radius ρ and wavelength λ. Thus its wavenumber is $k = 2\pi/\lambda$, its pitch angle β is given by $\cos\beta = [1 + (k\rho)^2]^{-1/2}$ and its equation is given in Eq. 8. It is connected to the head by a midpiece or proximal segment of length δ. The whole organism is translating with a velocity $\mathbf{w}$, the flagellum is rotating about the origin with an angular velocity Ω, and the head is rotating with the angular velocity Ω_H.

We assume that Ω_H differs from Ω only in the z component, so we write $\Omega = (\Omega_1, \Omega_2, \Omega_3)$ and $\Omega_H = (\Omega_1, \Omega_2, \omega_H)$. The difference $\omega_H - \Omega_3 = \omega$ is the angular frequency of the helical wave motion, which we assume to be given.

From Eqs. 19 and 20 we see that $\mathbf{F}^h$ and $\mathbf{T}^h$ are expressible in the form

$$\begin{pmatrix} \mathbf{F}^h \\ L^{-1}\mathbf{T}^h \end{pmatrix} = \frac{2\pi\mu L}{\log(b/\alpha L)} G^h \begin{pmatrix} \mathbf{w} \\ L\Omega \end{pmatrix}. \tag{31}$$

A lengthy calculation yields for the dimensionless sixth-order drag matrix G^h the result given in Appendix B.

The force and torque on the head about the origin are $-6\pi\mu R\mathbf{w}$ and $-8\pi\mu R^3\Omega_H + \mathbf{r}_H \times (-6\pi\mu R\mathbf{w})$, respectively, where $\mathbf{r}_H = (0, 0, z_H)$. The coordinate z_H of the center of the head is $-R(\delta^2 - \rho^2)^{1/2}$ if the proximal segment of length δ is a straight line (see Fig. 3). We shall not calculate the force and torque on this segment because we do not know its shape, and in any case they are small compared to those on the head and helix. They can be partly included in the force and torque on the head by appropriately adjusting R and z_H.

Now we add the force and torque on the head to those on the helix and equate the sums to zero, noting that

$$\Omega_H = \Omega + (0, 0, \omega). \tag{32}$$

Using Eq. 32 in 31 and transposing the term in ω to the right of the equation, we obtain

$$\frac{\pi\mu}{\log(b/\alpha L)} G^h \begin{pmatrix} \mathbf{w} \\ L\Omega \end{pmatrix} - 2\pi\mu R \begin{pmatrix} 3\mathbf{w} \\ 4L^{-1}R^2\Omega + 3L^{-1}\mathbf{r}_H \times \mathbf{w} \end{pmatrix} = 8\pi\mu \frac{R^3}{L} \begin{pmatrix} 0 \\ 0 \\ 0 \\ 0 \\ 0 \\ \omega \end{pmatrix}. \tag{33}$$

This equation is of the same form as Eq. 2 with $\mathbf{F}' = 0$ and $\mathbf{T}' = 8\pi\mu R^3(0, 0, \omega)$. Thus the torque on the head, due to the relative rotation with angular velocity ω, is needed to produce the swimming motion.

In order to solve Eq. 33 for $\mathbf{w}$ and Ω, we shall first simplify it for the case in which the helix length L is large compared with the other lengths, ρ, R, and λ. We shall keep all terms of order ρL^{-1} and $\rho^2 L^{-2}\log(b/L)$ and omit terms of order $\rho^2 L^{-2}$, $R^2 L^{-2}\log(b/\alpha L)$, and smaller, compared to unity. In doing so we anticipate that $\Omega_3/\omega = 0(1)$, $w_3/c = 0(1)$, $w_1/c = 0(\rho L^{-1})$, $w_2/c = 0(\rho L^{-1})$, $\Omega_1/\omega = 0(\rho^2 L^{-2})$, and $\Omega_2/\omega = 0(\rho^2 L^{-2})$. Here $c = \omega/k$ is the phase velocity of the wave along the helix. Upon using the expression for G^h given in Appendix B, we obtain in this way the following equations:

$$[2 - (k^2\rho^2/2)\cos^2\beta - 3(R/L)\log(b/\alpha L)]w_1 + (\rho/L)\cos\beta(1 - \cos\zeta)w_3 + \cos\beta[1 - (k^2\rho^2/4)\cos^2\beta]\Omega_2 L - (\rho/L\zeta)(2 - k^2\rho^2\cos^2\beta)(1 - \cos\zeta)\Omega_3 L = 0, \tag{34}$$

$$[2 - (k^2\rho^2/2)\cos^2\beta - 3(R/L)\log(b/\alpha L)]w_2 - (\rho/L)\cos\beta\sin\zeta w_3 - \cos\beta[1 - (k^2\rho^2/4)\cos^2\beta]\Omega_1 L + (\rho/L\zeta)(2 - k^2\rho^2\cos^2\beta)\sin\zeta\Omega_3 L = 0,$$

$$[2 - \cos^2\beta - (3R/L)\log(b/\alpha L)]w_3 - (k\rho^2/L)\cos^2\beta\Omega_3 L = 0,$$

$$-\cos\beta[1 - (k^2\rho^2/4)\cos^2\beta]w_2 + (\rho/L)\cos^2\beta\sin\zeta w_3 + \tfrac{2}{3}\cos^2\beta[1 - (k^2\rho^2/4)\cos^2\beta]\Omega_1 L - (\rho\sin\zeta/kL^2)(2 - k^2\rho^2\cos^2\beta)\Omega_3 L = 0,$$

$$\cos\beta[1 - (k^2\rho^2/4)\cos^2\beta]w_1 - (\rho/L)\cos^2\beta\cos\zeta w_3$$
$$+ \tfrac{2}{3}\cos^2\beta[1 - (k^2\rho^2/4)\cos^2\beta]\Omega_2 L + (\rho\cos\zeta/kL^2)(2 - k^2\rho^2\cos^2\beta)\Omega_3 L = 0,$$
$$-(k\rho^2/L)\cos^2\beta w_3 + [(2\rho^2/L^2) - (\rho^4/L^4)\zeta^2 - (4R^3/L^3)\log(b/\alpha L)]\Omega_3 L$$
$$= (4\omega R^3/L^2)\log(b/\alpha L).$$

Here $\zeta = kL\cos\beta$.

The solution of the third and sixth equations for w_3 and Ω_3 is

$$w_3/c = (k^2\rho^2/D)(4R^3/L^3)\log(b/\alpha L), \tag{35}$$

$$\Omega_3/\omega = (4R^3/DL^3)\log(b/\alpha L)[1 + 2k^2\rho^2 - (1 + k^2\rho^2)3(R/L)\log(b/\alpha L)]. \tag{36}$$

Here D is defined by

$$D = (\rho^2/L^2)[2(1 + k^2\rho^2) - (2 + k^2\rho^2)(3R/L)\log(b/\alpha L)]$$
$$- (4R^3/L^3)\log(b/\alpha L)[1 + 2k^2\rho^2 - (1 + k^2\rho^2)(3R/L)\log(b/\alpha L)]. \tag{37}$$

The remaining equations then yield

$$w_1/c = 16\rho R^3 L^{-4}\log(b/\alpha L)(1 + k^2\rho^2)^{3/2}(2 + \cos\zeta)N$$
$$/[4 + 3k^2\rho^2 - 24(1 + k^2\rho^2)RL^{-1}\log(b/\alpha L)]D$$
$$w_2/c = 16\rho R^3 L^{-4}\log(b/\alpha L)(1 + k^2\rho^2)^{3/2}N\sin\zeta$$
$$/[4 + 3k^2\rho^2 - 24(1 + k^2\rho^2)RL^{-1}\log(b/\alpha L)]D$$
$$= [\sin\zeta/(2 + \cos\zeta)](w_1/c),$$
$$\Omega_1/\omega = 48\rho R^3 k^{-1}L^{-5}\log(b/\alpha L)(1 + k^2\rho^2)^2 N\sin\zeta[4 + 3k^2\rho^2$$
$$- 12(1 + k^2\rho^2)RL^{-1}\log(b/\alpha L)]$$
$$/[4 + 3k^2\rho^2 - 24(1 + k^2\rho^2)RL^{-1}\log(b/\alpha L)](4 + 3k^2\rho^2)D \tag{38}$$
$$= \{3(1 + k^2\rho^2)^{1/2}[4 + 3k^2\rho^2 - 12(1 + k^2\rho^2)RL^{-1}\log(b/\alpha L)]$$
$$/kL(4 + 3k^2\rho^2)\}(w_2/c),$$
$$-\Omega_2/\omega = -48\rho R^3 k^{-1}L^{-5}\log(b/\alpha L)(1 + k^2\rho^2)^2 N[(4 + 3k^2\rho^2)(1 + \cos\zeta)$$
$$- 12(1 + k^2\rho^2)\cos\zeta RL^{-1}\log(b/\alpha L)]$$
$$/[4 + 3k^2\rho^2 - 24(1 + k^2\rho^2)RL^{-1}\log(b/\alpha L)](4 + 3k^2\rho^2)D$$
$$= -\{3(1 + k^2\rho^2)^{1/2}[(4 + 3k^2\rho^2)(1 + \cos\zeta)$$
$$- 12(1 + k^2\rho)\cos\zeta RL^{-1}\log(b/\alpha L)]/kL(2 + \cos\zeta)(4 + 3k^2\rho^2)\}(w_1/c).$$

The quantity N is defined by

$$N = 2(1 + k^2\rho^2) - (2 + k^2\rho^2)(3R/L)\log(b/\alpha L). \tag{39}$$

These results confirm the order of magnitude assumptions made in simplifying Eq. 33.

Corresponding to the expression for the angular velocity of the tail (Eq. 36), the expression for the z component ω_H of the angular velocity of the head Ω_H is given, with the aid of Eq. 32, as

$$\omega_H/\omega = (\rho^2/L^2D)[2(1 + k^2\rho^2) - (2 + k^2\rho^2)(3R/L)\log(b/\alpha L)]. \quad (40)$$

Eqs. 35 and 40 are in agreement with those given by Chwang and Wu (1971). Comparison of Eqs. 36 and 40 shows that the direction of rotation of the tail is opposite to that of the head. We note in Eq. 36 that the quantity $\log(b/\alpha L)$ is a negative number because $b/L \ll 1$, so that in general Ω_3 never vanishes for $R > 0$.

Our results (Eqs. 35 and 36) for w_3 and Ω_3 agree exactly with the corresponding results of Chwang and Wu (1971) when their small term of order b^2/ρ^2 is omitted, provided we set $\alpha = 2e^{-1/2}\lambda/L$. This is just the choice made by Gray and Hancock in defining the tangential drag coefficient C_s, which Chwang and Wu used. This agreement shows that their formula is correct when terms of order ρ^2L^{-2}, $R^3L^{-2}\log(b/\alpha L)$, and smaller are neglected. An improved formula for this case, valid when such terms are not small, can be obtained by solving the equation system 33 in conjunction with the matrix G^h given in Appendix B. We shall not give this explicit solution here. They have also carefully examined some of the consequences of the results for w_3 and Ω_3, including the determination of the optimum ratio R/b of head radius to flagellum radius for maximum speed w_3. They have shown that this optimum ratio is in general agreement with the values observed on some bacterial flagella.

If we omit terms of orders ρ/L and $\rho^2L/R^3\log(b/\alpha L)$ from Eqs. 34–39 we get

$$w_3/c = -k^2\rho^2/[1 + 2k^2\rho^2 - 3RL^{-1}\log(b/\alpha L)(1 + k^2\rho^2)], \quad \Omega_3 = -\omega,$$
$$w_1 = w_2 = \Omega_1 = \Omega_2 = \omega_H = 0. \quad (41)$$

When we use the above value of α in this result for w_3, it becomes the result of Holwill and Burge (1963). We note the meaning of the negative signs in Eq. 41, as follows. A helical wave with left-handed chirality (see Fig. 4) propagating in the positive z direction is equivalent to a counterclockwise rotation of the tail (viewed distally). Such motion produces a propulsive velocity w_3 which is in the negative z direction. When we omit the term $RL^{-1}\log(b/\alpha L)$, Eq. 41 reduces to Hancock's (1953) result

$$w_3/c = -k^2\rho^2/(1 + 2k^2\rho^2). \quad (42)$$

For $k^2\rho^2 \ll 1$, this simplifies to Taylor's (1952) formula

$$w_3/c = -k^2\rho^2.$$

Chwang and Wu (1971) have pointed out that when the head radius R alone tends to zero, then w_3 tends to zero, as Eq. 35 shows. Thus Hancock's result (Eq. 42) is not obtained in this limit. However, as we have just demonstrated, if ρ/L and b/L also tend to zero in such a way that $\rho^2L/R^3\log(b/\alpha L)$ and $RL^{-1}\log(b/\alpha L)$ tend to zero, then Eq. 42 is obtained. Therefore it is in this limit that Eq. 42 holds.

The theory of Cox (1971) shows that the quantity α, which we have introduced in

Eqs. 19 and 20, is determined by the term of order $(\log b/L)^{-2}$ in the velocity field. Thus it depends upon the shape and motion of the entire body. Therefore the force at each point on the body is not just equal to a drag coefficient matrix multiplied by the velocity of the body at that point, as Gray and Hancock (1955) assume. Instead it also depends upon the flow velocity induced by the rest of the body, as Cox has shown. Although α can be calculated from his formulas, we shall not evaluate it in this paper. It has been calculated by Shack et al. (1974), ignoring rotation.

We have compared Eqs. 36 and 40 with the observations of Rikmenspoel et al. (1960). Rikmenspoel (1965) represented the tail motion as a sum of two sinusoidal terms, one of which had an amplitude about two or three times that of the other. He inferred the mean translational velocity and the mean frequencies of oscillation of the head and tail, respectively, to be

$$v \sim 100\,\mu\text{m/s}, \qquad f_H \sim 9/\text{s}, \qquad f_T \sim 13/\text{s}.$$

The translational velocity is about the same as that reported by Gray (1958). We identify the quantity v as w_3, f_H as $\omega_H/2\pi$, and the quantity $(-f_T)$ as $\Omega_3/2\pi$. We choose the following typical values of the required parameters:

$$\rho = 7\,\mu\text{m}, \quad b = 0.4\,\mu\text{m}, \quad R = 4\,\mu\text{m},$$
$$k = 0.1/\mu\text{m}, \quad L = 50\,\mu\text{m}.$$

From Eq. 32 we infer that $\omega \sim 140/\text{s}$ and therefore $c \sim 1{,}400\,\mu\text{m/s}$. Then, from Eqs. 35, 36, and 40, with α as before, we compute

$$v = w_3 = 47\,\mu\text{m/s},$$
$$f_H = \omega_H/2\pi = 14/\text{s},$$
$$f_T = -\Omega_3/2\pi = 9.6/\text{s}.$$

The agreement with observation is at best fair. The disagreement may be due to the difference between the actual motion of the tail, reported by Rikmenspoel (1965), and our assumed helical motion. Another contributing factor may be the neglect of various higher order terms in the theory. It is to be hoped that further quantitative studies of the flagellar motion will clarify the true nature of the motion and lead to closer agreement between theory and observation.

Dr. Rubinow is also affiliated with Sloan-Kettering Institute for Cancer Research, New York.

This work was supported in part by the National Science Foundation under grant GP-32996X3 and grant MPS74-19234.

Received for publication 21 May 1975 and in revised form 10 September 1975.

REFERENCES

BROKAW, C. J. 1965. Non-sinusoidal bending waves of sperm flagella. *J. Exp. Biol.* **43**:155.

BROKAW, C. J. 1970. Bending moments in free-swimming flagella. *J. Exp. Biol.* **53**:445.

BROKAW, C. J. 1971. Bend propagation by a sliding filament model for flagella. *J. Exp. Biol.* **55**:289.

BULLER, A. H. R. 1903. Is chemotaxis a factor in the fertilization of the eggs of animals? *Q. J. Microsc. Sci.* **46**:154.

CHWANG, A. T., and T. Y. WU. 1971. A note on the helical movement of micro-organisms. *Proc. R. Soc. Lond. B Biol. Sci.* **178**:327.
COX, R. G. 1970. The motion of long slender bodies in a viscous fluid. *J. Fluid Mech.* **44**:791.
GOLDSTEIN, H. 1950. Classical Mechanics. Addison-Wesley Publishing Co. Ltd., London. Chapter 4.
GRAY, J. 1955. The movement of sea-urchin spermatozoa. *J. Exp. Biol.* **32**:775.
GRAY, J. 1958. The movement of the spermatozoa of the bull. *J. Exp. Biol.* **35**:96.
GRAY, J., and G. J. HANCOCK. 1955. The propulsion of sea-urchin spermatozoa. *J. Exp. Biol.* **32**:802.
HANCOCK, G. J. 1953. Self-propulsion of microscopic organisms through liquids. *Proc. R. Soc. Lond. A Phys. Sci.* **217**:96.
HOLWILL, M. E. J., and R. E. BURGE. 1963. A hydrodynamic study of the motility of flagellated bacteria. *Arch. Biochem. Biophys.* **101**:249.
RIKMENSPOEL, R. 1965. The tail movement of bull spermatozoa. Observations and model calculations. *Biophys. J.* **5**:365.
RIKMENSPOEL, R., G. VAN HERPEN, and P. EIJKHOUT. 1960. Cinematographic observations of the movements of bull sperm cells. *Phys. Med. Biol.* **5**:167.
ROTHSCHILD, LORD, and M. M. SWANN. 1949. The fertilization reaction in the sea-urchin egg. *J. Exp. Biol.* **26**:164.
ROTHSCHILD, LORD, and M. M. SWANN. 1950. The fertilization reaction in the sea-urchin egg. The effect of nicotine. *J. Exp. Biol.* **27**:400.
SHACK, W. J., C. S. FRAY, and T. J. LARDNER. 1974. Observations on the hydrodynamics and swimming motions of mammalian spermatozoa. *Bull. Math. Biol.* **36**:555.
TAYLOR, G. I. 1952. The action of waving cylindrical tails in propelling microscopic organisms. *Proc. R. Soc. Lond. A Phys. Sci.* **211**:225.
YUNDT, A. P., W. J. SHACK, and T. J. LARDNER. 1975. Applicability of hydrodynamic analyses of spermatozoan motion. *J. Exp. Biol.* **62**:27.

APPENDIX A

We now calculate the drag matrix G^p, as well as the relative force and torque, in the planar case, using Eqs. 19–23. The coefficient of $(\mathbf{w},\Omega)$ in the result for $(\mathbf{F},\mathbf{T})$ is $2\pi\mu L[\log(b/\alpha L)]^{-1}G^p$, and the remaining terms yield $\mathbf{F}^r$ and $\mathbf{T}^r$.

After straightforward calculation, in which terms of order ϵ are omitted, we find the following results for G^p:

$$G^p_{11} = 3 - G^p_{22} = 1 + \frac{1}{kL}\int_{-\omega t}^{\theta_1}(1 + k^2\rho^2\sin^2\theta)^{-1/2}d\theta$$

$$G^p_{12} = G^p_{21} = \frac{\rho}{L}\int_{-\omega t}^{\theta_1}\sin\theta(1 + k^2\rho^2\sin^2\theta)^{-1/2}d\theta$$

$$G^p_{13} = G^p_{31} = \frac{ct}{L} + \frac{1}{k^2L^2}\int_{-\omega t}^{\theta_1}\theta(1 + k^2\rho^2\sin^2\theta)^{1/2}d\theta$$

$$+ \frac{1}{k^2L^2}\int_{-\omega t}^{\theta_1}(\theta + \omega t)(1 + k^2\rho^2\sin^2\theta)^{-1/2}d\theta$$

$$+ \frac{1}{k^2L^2}[(1 + k^2\rho^2\sin^2\omega t)^{1/2} - (1 + k^2\rho^2\sin^2\theta_1)^{1/2}]$$

$$G^p_{23} = G^p_{32} = -\frac{2\rho}{kL^2}\int_{-\omega t}^{\theta_1}\cos\theta(1 + k^2\rho^2\sin^2\theta)^{1/2}d\theta$$

$$+ \frac{\rho}{kL^2}\int_{-\omega t}^{\theta_1}[(\theta + \omega t)\sin\theta + \cos\theta](1 + k^2\rho^2\sin^2\theta)^{-1/2}d\theta$$

$$G^p_{33} = \frac{1}{kL^3}\int_{-\omega t}^{\theta_1}\left\{\frac{2}{k^2}([\theta+\omega t]^2 + k^2\rho^2\cos^2\theta)(1+k^2\rho^2\sin^2\theta)^{1/2} - \rho^2([\theta+\omega t]\sin\theta+\cos\theta)^2(1+k^2\rho^2\sin^2\theta)^{-1/2}\right\}d\theta$$

$$= \frac{1}{k^3L^3}\int_{-\omega t}^{\theta_1}\{([\theta+\omega t]^2 + 2k^2\rho^2\cos^2\theta)(1+k^2\rho^2\sin^2\theta)^{1/2} + ([\theta+\omega t]^2 - k^2\rho^2\cos^2\theta)(1+k^2\rho^2\sin^2\theta)^{-1/2}\}d\theta + \frac{2}{k^2L^3}[L - z_1(1+k^2\rho^2\sin^2\theta_1)^{1/2}].$$

The other elements of G^p are zero. Here $\theta_1 = kz_1 - \omega t$ where z_1 is determined by Eq. 5 with $s = L$.

The nonzero components of $\mathbf{F}^r$ and $\mathbf{T}^r$ are:

$$F^r_1 = \frac{2\pi\mu L}{\log(b/\alpha L)}\left\{\frac{\rho c}{L}(\cos\omega t - \cos\theta_1)(1+k^2\rho^2\sin^2\omega t)^{1/2} + \frac{\rho c}{L}\int_{-\omega t}^{\theta_1}\sin\theta(1+k^2\rho^2\sin^2\theta)^{-1/2}d\theta\right\}$$

$$F^r_3 = \frac{2\pi\mu L}{\log(b/\alpha L)}\left\{2c - \frac{cz_1}{L}(1+k^2\rho^2\sin^2\omega t)^{1/2} - \frac{c}{kL}\int_{-\omega t}^{\theta_1}(1+k^2\rho^2\sin^2\theta)^{-1/2}\mathrm{d}\theta\right\}$$

$$L^{-1}T_2 = \frac{2\pi\mu L}{\log(b/\alpha L)}\left\{-\frac{2\rho c}{kL}\int_{-\omega t}^{\theta_1}(1+k^2\rho^2\sin^2\theta)^{1/2}\cos\theta\,\mathrm{d}\theta + \frac{c\rho}{kL}\int_{-\omega t}^{\theta_1}(1+k^2\rho^2\sin^2\theta)^{-1/2}[(\theta+\omega t)\sin\theta+\cos\theta]\mathrm{d}\theta + \frac{c\rho}{kL}(1+k^2\rho^2\sin^2\omega t)^{1/2}(2\sin\theta_1 + 2\sin\omega t - kz_1\cos\theta_1)\right\}.$$

APPENDIX B

The drag matrix G^h for a helix can be calculated by substituting into Eqs. 19 and 20 the equations for a helix and for its velocity. These are

$$\mathbf{r}(s) = (\rho\cos\theta, \rho\sin\theta, k^{-1}\theta),$$

$$\mathbf{v}(s) = \mathbf{w} + \Omega\times\mathbf{r}(s) = (w_1 + \Omega_2k^{-1}\theta - \Omega_3\rho\sin\theta,\ w_2 + \Omega_3\rho\cos\theta - \Omega_1k^{-1}\theta,\ w_3 + \Omega_1\rho\sin\theta - \Omega_2\rho\cos\theta),$$

where $\theta = ks\cos\beta$. From the above equation for $\mathbf{r}(s)$ we have

$$\mathbf{dr}(s)/\mathrm{d}s = \cos\beta(-k\rho\sin\theta, k\rho\cos\theta, 1).$$

To illustrate the method of calculation, we shall evaluate G^h_{11} by substituting the last two equations into 19. The coefficient of w_1 in the equation for F^h_1 is found to be, with $\zeta = kL\cos\beta$,

$$G^h_{11} = \frac{1}{\zeta}\int_0^{\zeta}(2 - k^2\rho^2\cos^2\beta\sin^2\theta)\,d\theta$$

$$= 2 - \frac{\rho^2\zeta}{4L^2}(2\zeta - \sin 2\zeta).$$

In a similar way we find that G^h is a symmetric matrix, the remaining elements of which are:

$$G^h_{12} = G^h_{21} = (\rho^2\zeta/4L^2)(1 - \cos 2\zeta),$$

$$G^h_{13} = G^h_{31} = (\rho/L)\cos\beta(1 - \cos\zeta),$$

$$G^h_{14} = G^h_{41} = (\rho^2/8L^2)\cos\beta(4\zeta + 2\zeta\cos 2\zeta - 3\sin 2\zeta),$$

$$G^h_{15} = G^h_{51} = \cos\beta[1 - (\rho^2/8L^2)(3 - 3\cos 2\zeta + 2\zeta^2 - 2\zeta\sin 2\zeta)],$$

$$G^h_{16} = G^h_{61} = [-(2\rho/L\zeta) + (\rho^3\zeta/L^3)](1 - \cos\zeta),$$

$$G^h_{22} = 2 - (\rho^2\zeta/4L^2)(2\zeta + \sin 2\zeta),$$

$$G^h_{23} = G^h_{32} = -(\rho/L)\cos\beta\sin\zeta,$$

$$G^h_{24} = G^h_{42} = -\cos\beta[1 + (\rho^2/8L^2)(3 - 3\cos 2\zeta - 2\zeta^2 - 2\zeta\sin 2\zeta)],$$

$$G^h_{25} = G^h_{52} = (\rho^2\cos\beta/8L^2)(4\zeta + 3\sin 2\zeta - 2\zeta\cos 2\zeta),$$

$$G^h_{26} = G^h_{62} = [(2\rho/L\zeta) - (\rho^3\zeta/L^3)]\sin\zeta,$$

$$G^h_{33} = 2 - \cos^2\beta,$$

$$G^h_{34} = G^h_{43} = (\rho/L\zeta)[2 - 2\cos\zeta - \cos^2\beta(2 - 2\cos\zeta - \zeta\sin\zeta)],$$

$$G^h_{35} = G^h_{53} = (\rho/L\zeta)[-2\sin\zeta + \cos^2\beta(2\sin\zeta - \zeta\cos\zeta)],$$

$$G^h_{36} = G^h_{63} = -(\rho^2/L^2)\zeta\cos\beta,$$

$$G^h_{44} = \tfrac{2}{3}\cos^2\beta + (\rho^2/L^2)\{1 - (\sin 2\zeta/2\zeta) - (\cos^2\beta/8)[4 - (5\sin 2\zeta/\zeta) + 2\zeta\sin 2\zeta + 6\cos 2\zeta + \tfrac{4}{3}\zeta^2]\},$$

$$G^h_{45} = G^h_{54} = (\rho^2/8L^2\zeta)[-4 + 4\cos 2\zeta + \cos^2\beta(5 - 5\cos 2\zeta - 6\zeta\sin 2\zeta + 2\zeta^2\cos 2\zeta)],$$

$$G^h_{46} = G^h_{64} = (\rho/kL^2)\{[(2 - 2\cos\zeta)/\zeta] - 2\sin\zeta + (\rho^2\zeta/L^2)\cdot(-2 + 2\cos 2\zeta + \zeta\sin\zeta)\},$$

$$G^h_{55} = \tfrac{2}{3}\cos^2\beta + (\rho^2/L^2)\{1 + (\sin 2\zeta/2\zeta) - (\cos^2\beta/8)[4 + (5\sin 2\zeta/\zeta) - 2\zeta\sin 2\zeta - 6\cos 2\zeta + \tfrac{4}{3}\zeta^2]\},$$

$$G^h_{56} = G^h_{65} = (\rho/kL^2)[2\cos\zeta - (2\sin\zeta/\zeta) + (\rho^2\zeta/L^2)(2\sin\zeta - \zeta\cos\zeta)],$$

$$G^h_{66} = (2\rho^2/L^2) - (\rho^4\zeta^2/L^4).$$